2006

Dehydrogenation mechanism in catalyst-activated MgH2

S. Li
Virginia Commonwealth University

Puru Jena
Virginia Commonwealth University, pjena@vcu.edu

R. Ahuja
Uppsala Universitet

Li, S., Jena, P., Ahuja, R. Dehydrogenation mechanism in catalyst-activated MgH2. Physical Review B, 74, 132106 (2006).

Dehydrogenation mechanism in catalyst-activated MgH_2

S. Li and P. Jena
Physics Department, Virginia Commonwealth University, Richmond, Virginia 23284-2000, USA

R. Ahuja
Condensed Matter Theory Group, Department of Physics, Uppsala University, Box 530, SE 751 21 Uppsala, Sweden

(Received 31 May 2006; revised manuscript received 30 June 2006; published 26 October 2006)

A small amount of Nb_2O_5 catalyst is known to substantially improve the desorption thermodynamics and kinetics of MgH_2. Using density functional theory in combination with *ab initio* molecular dynamics simulation, we provide theoretical understanding of the mechanism of dehydrogenation in Nb doped MgH_2. We show that the substitution of Nb at the Mg site followed by the clustering of H around Nb is a likely pathway for hydrogen desorption. We also find that dehydrogenation from the vicinity of Mg vacancies is exothermic. However, the vacancies are not likely to play a significant role in hydrogen desorption due to their high formation energy (3.87 eV).

DOI: 10.1103/PhysRevB.74.132106 PACS number(s): 81.05.Zx, 68.43.Bc, 71.15.Nc

Due to the rising standards of living and growing population worldwide, global energy consumption is expected to increase dramatically. Hydrogen has been projected as a long-term solution for a secure energy resource. However, the success of a hydrogen economy relies on our ability to store hydrogen safely and economically under ambient conditions and with large gravimetric and volumetric density. Although lightweight metal hydrides such as MgH_2 meet the economic as well as gravimetric and volumetric density requirements, their kinetics and thermodynamics are not favorable. Thus, catalysts are needed so that the storage systems can operate under moderate conditions. In spite of a considerable amount of experimental work studying the role of different catalysts on hydrogen desorption in MgH_2, no conclusive picture regarding its mechanism has emerged. In this paper we provide such an understanding by carrying out comprehensive theoretical studies of the role of Nb substitution and vacancies on hydrogen bonding and desorption. The role of metal substitution on hydrogen adsorption on the $Mg(00\bar{1}1)$ surface[1] will be discussed in a forthcoming paper.

It is known that MgH_2 contains 7.6 wt. % of hydrogen and can remain stable even up to 300 °C.[2] Several attempts have been made in order to improve the hydriding-dehydriding kinetics and thermodynamics of MgH_2. These experiments fall into three categories, Liang and co-workers[3] studied the role of metal additives on hydrogen adsorption/desorption while Klassen and co-workers[4,5] concentrated on metal oxide additives. Zaluska *et al.*,[6,7] on the other hand, studied both types of additives. Subsequent experimental works have followed this trend. In all these approaches, hydriding-dehydriding kinetics improved and hydrogen desorption temperature decreased although the underlying mechanism is unknown. Pelletier *et al.*[8] suggested that the improved kinetics in Nb doped MgH_2 is due to the formation of niobium-hydride. Shang *et al.*[9] reported that the (MgH_2 +Ni) mixture gives the highest level of hydrogen desorption and the most rapid kinetics at 300 °C under vacuum, followed by alloys of Al, Fe, Nb, Ti, and Cu. They attributed the kinetic improvements to metal atom substitution. Oelerich *et al.*[4,10,11] studied the catalytic effects of metal oxides (M_xO_y) on the hydrogen sorption in nanocrystalline MgH_2 Fe_3O4 was found to be the best candidate and MgH_2/M_xO_y powders were observed to release hydrogen even at 200 °C, Barkhordarian *et al.*[12] compared Nb_2O_5 to other metal oxide catalysts including Fe_3O_4. Their results demonstrated that the catalytic effect of Nb_2O_5 is superior in absorption as well as desorption. A year later, they reported that the fastest kinetics is obtained when using 0.5 mole % Nb_2O_5 at temperatures of 250 °C and 300 °C.[13] Recently, Fatay *et al.*[14] investigated the effect of milling time and grain size on the hydrogen desorption temperature and on the dehydriding kinetics of ball-milled ($MgH_2+Nb_2O_5$) powders. They reported that the grain-size reduction substantially decreases the hydrogen desorption temperature. Catalyst was observed to lower the activation energy of dehydriding after about 15 min of ball milling and this effect is suppressed at longer milling times. They hypothesized the mechanism as immediate penetration of the catalytic particles into the MgH_2 during ball milling.

Theoretical studies aimed at explaining the role of catalysts in hydrogen sorption in MgH_2 are limited. Recently first-principles calculations on MgH_2-M (M=Al, Ti, Fe, Ni, Cu, or Nb) alloys have been performed to study the effect of alloying elements on the stability and electronic structure of MgH_2.[15,16] Although these studies suggested that the destabilization of MgH_2 by the alloying elements is due to the Mg-H bond weakening, no attempt has been made to calculate the actual energy needed to remove a H atom nor the influence H removal has on the crystal structure. Thus, a fundamental understanding of how the catalyst works has remained unattainable.

There are several ways Nb_2O_5 can help in lowering the desorption temperature: First, Nb_2O_5 can react with MgH_2 and form MgO, metallic Nb and H_2 according to the following reaction:

$$2Nb_2O_5 + 10MgH_2 = 10MgO + 4Nb + 10H_2, \quad (1)$$

the Nb atom can replace a Mg atom and locally change the electronic structure of the hydride. Second, since MgO_x[16] has been observed in the reaction products, one could assume that this formation may leave some Mg vacancies in the sample, which may affect H desorption. Third, $(Nb,Mg)O_x$ complex can form during ball milling and this formation could lead to the weakening of the Mg-H bond as suggested by Dehouche *et al.*[17] and Friedrichs *et al.*[18] Fourth, different

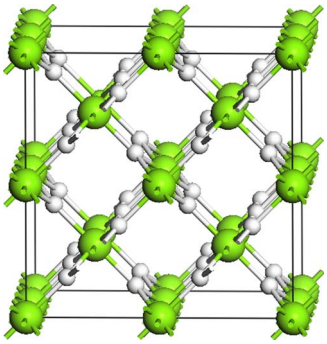

FIG. 1. (Color online) The 48-atom ($2\times2\times2$) supercell geometry of MgH_2. The green (gray) and white color atoms correspond to Mg and H, respectively.

phases such as Nb hydride (NbH_x, $x<1.0$), $(Nb,Mg)H_x$ solid solution may exist in the ball-milled mixture and may be responsible for the improved dehydrogenation behavior.[19,20] To gain a fundamental understanding of the role of the Nb based catalyst on dehydrogenation, we have carried out a series of first-principles calculations using supercell band structure method. We have examined the effect of Nb substitution as well as the Mg vacancies on the hydrogen bonding and the dehydrogenation mechanism.

The electronic structure of MgH_2 was first studied by constructing a ($2\times2\times2$) supercell consisting of 48 atoms ($Mg_{16}H_{32}$) (see Fig. 1). To simulate a vacancy or Nb substitution at the Mg 2*a* site (0.5, 0.5, 0.5), we created $Mg_{15}H_{32}$ and $(NbMg_{15})H_{32}$ supercells, respectively. The optimized structure, energetics, and electronic structure were carried out using generalized gradient approximation (GGA) (Ref. 21) in the density functional theory (DFT) (Ref. 22) and the projector augmented wave (PAW) (Ref. 23) method. The PAW potentials with the valence states 3*s* and 3*p* for Mg; 4*p*, 4*d*, and 5*s* for Nb; and 1*s* for H were used as prescribed in the Vienna *ab initio* simulation package (VASP).[24] High precision calculations with a cutoff energy of 500 eV for the plane-wave basis were performed. The geometries of the above supercells (ionic coordinates and c/a ratio) were optimized without any symmetry constraint. For the sampling of the irreducible wedge of the Brillouin zone we used *k*-point grids of $4\times4\times4$ for the geometry optimization and cohesive energy calculations at the equilibrium volume. In all calculations, self-consistency was achieved with a tolerance in the total energy of at least 1 meV. Hellman-Feynman force components on each ion in the supercells are converged to 5 meV/Å. To determine the energy to remove a H atom from pure MgH_2 as well as from that containing either a vacancy or substitutional Nb atom, we repeated all of the above calculations with $Mg_{16}H_{31}$, $Mg_{15}H_{31}$, and $(NbMg_{15})H_{31}$ supercells. The accuracy of our method is confirmed by comparing the calculated cohesive energy of 1.53 eV/atom for Mg metal (hexagonal close-packed structure) with the corresponding experimental value of 1.51 eV/atom.[25] The cohesive energy of Nb metal (body-centered cubic structure) is 7.07 eV/atom in comparison with corresponding experimental value of 7.57 eV/atom.[25] Similarly, the calculated binding energy of 4.56 eV for a H_2 molecule agrees well with the experimental value of 4.75 eV.[26]

To examine if the optimized geometries of the supercells correspond to local minima in the potential energy surface, *ab initio* molecular dynamics (MD) simulations were carried at 300 K for $Mg_{16}H_{31}$, $(NbMg_{15})H_{32}$, $(NbMg_{15})H_{31}$, and $Mg_{15}H_{32}$ supercells. One thousand time steps, each 1 fs long, were chosen for equilibration.[27] The velocities were scaled at each time step. The final MD-relaxed geometries are further relaxed by a total energy minimization scheme.[28] In the following we discuss our results.

MgH_2 crystallizes in the tetragonal structure ($P4_2/mnm$) at ambient conditions. Our calculated lattice constants $a=4.495$ Å and $c=3.005$ Å of the primitive cell compare very well with the corresponding experimental values of 4.501 Å and 3.01 Å.[29] In MgH_2, Mg occupies the 2*a* site and H occupies the 4*f* site with $x=0.304$.[30] Each Mg atom is octahedrally coordinated to H atoms with two H atoms lying along [110] direction at a distance of 1.935 Å while the other four H atoms on the (110) plane lie at a distance of 1.951 Å. Each H atom is bonded to three Mg atoms. The calculated density of states (DOS) of MgH_2 is presented in Fig. 2(a). From the total DOS we see that MgH_2 is an insulator characterized by a band gap of 4.0 eV. The insulating behavior originates mainly from the ionic bonding characteristics between Mg^{2+} and H^-. The valence band is dominated by H-*s* states and the conduction band mainly consists of Mg *s* and *p* states. However, a small amount of Mg s and *p* states in the valence band hybridize with the H *s* states and contribute some covalent character to the bonding. Hydrogen atoms (marked *A* and *B* in Fig. 3) are not equivalent, even though these two H atoms belong to the same symmetry group, as their distances to the Mg atom are slightly different.[31] However, we note that the partial DOS of H atoms (marked *A* and *B* in Fig. 3) are nearly the same, suggesting that the electronic structure of these H atoms are not affected due to small difference in their distances from the Mg atom.

We then replaced one Mg atom at the 2*a* (0.5, 0.5, 0.5) site with a Nb atom [see Fig. 3(d)]. Similar to the case of MgH_2, the Nb atom is coordinated to six hydrogen atoms. Two of these H atoms along [110] direction are at a distance of 1.927 Å from the Nb atom while the other four lying on the (110) plane are at a distance of 1.932 Å. Each of these six hydrogen atoms is bonded to one Nb atom and two Mg atoms. The corresponding Mg-H bond length increases by about 0.1 Å and the H atoms come closer to the Nb atom, which shows that Nb has higher affinity to hydrogen than Mg. The calculated DOS of $(NbMg_{15})H_{32}$ is shown in Fig. 2(b). The Nb *d* states lie at the Fermi level and lend some metallic character to the system. There is a weak coupling between the H *s* and Nb *d* states in the valence band. We should point out that two H atoms *A* and *B* bound to Nb have different density of states as seen from Fig. 2(b). The *s* states of hydrogen atom *A* are found to hybridize more strongly with Nb d states than that of hydrogen atom *B*. This difference results from Nb *d*-orbital splitting in an octahedral symmetry.

The energy costs to remove H atoms from intrinsic MgH_2 as well from that when Nb is substituted at the Mg site are calculated by using the following equation:

$$\Delta E = E(\mathrm{Nb}_x\mathrm{Mg}_{16-x}\mathrm{H}_{32-n})_{\mathrm{coh}} - E(\mathrm{Nb}_x\mathrm{Mg}_{16-x}\mathrm{H}_{32})_{\mathrm{coh}} + n/2E(\mathrm{H}_2). \quad (2)$$

Here the indices x and n refer, respectively, to the number of Nb and H atoms in the supercell that are removed and E refers to the cohesive energy at 0 K defined with respect to the dissociated atoms. We find that it costs 1.6 eV to remove a hydrogen atom [either A or B in Fig. 3(a)], and 2.9 eV to remove two hydrogen atoms from the vicinity of the same Mg atom in pure MgH_2. In Nb doped MgH_2, the energy cost to remove one H atom (see H atom marked A and colored aqua) in Fig. 3(e) is 1.48 eV at 0 K, which is only marginally less than that from pure MgH_2. In contrast, the energy cost to remove one H atom lying on the (110) plane (marked B and colored blue) in Fig. 3(f) is −0.11 eV. This dramatic decrease in energy originates from structural changes following hydrogen removal from different positions. From Fig. 3(e) we see that removal of hydrogen atom A do not have much effect on the local structure around the Nb atom, while upon the removal of H atom B, two more hydrogen atoms from the second nearest neighbor configuration lying at a distance of 3.49 Å [see Fig. 3(f)] bind to the Nb atom. The energy gain due to the binding of this H pair is responsible for the lower energy cost for H dehydrogenation. The fact that this local distortion around Nb site was not seen in Fig. 3(e) suggests that the kinetic barrier for H motion along the [110] direction is higher than that in the (110) plane. To probe this further, we carried out molecular dynamics simulations at 300 K. At this temperature, Nb was found to bind to two more hydrogen atoms from its second nearest neighbor as in Fig. 3(f) and the energy cost to remove the H atom marked A reduced to 0.29 eV. In contrast, the energy cost to remove one hydrogen atom from pure MgH_2 [Figs. 3(b) and 3(c)] remains unchanged at 300 K. The significant lower energy cost in Nb substituted MgH_2 is due to clustering of H around of Nb after the removal of the first H atom. To analyze the dehydrogenation pathway due to Nb substitution, we removed four hydrogen H atoms from the plane. As these H atoms were removed, other four H atoms from the second-nearest-neighbor configuration were found to bind to the Nb atom. Note that Nb has eight second-nearest H atoms at distances between 3.5–3.6 Å and eight third-nearest H atoms at a distance of 4.0 Å. Thus, one can visualize the Nb atom to serve as a magnet that continues to attract nearby H atoms as the nearest ones are successively desorbed.

Pelletier *et al.*[8] have pointed out that that the improved kinetics in MgH_2-Nb may be due to high density defects, although the nature of these defects was not identified. Since, MgO has been found to form during ball milling of MgH_2 with Nb_2O_5, we studied the role of Mg vacancies on hydrogen desorption. We repeated the above calculations by using $Mg_{15}H_{32}$ and $Mg_{15}H_{31}$ supercells which simulate a Mg vacancy. Once a Mg vacancy is created, each of the six hydrogen atoms in the vicinity of the Mg vacancy, originally bound to three Mg atoms, is now more strongly bound to the remaining two nearest Mg atoms. No hydrogen molecule formation is observed during 0 K optimization. To check whether there are energy barriers that cannot be overcome at 0 K during dehydrogenation, we increased the temperature up to 300 K. Molecular hydrogen formation is observed only after 200 steps (200 fs). Two H atoms are found to bind to each other at a distance of 0.76 Å. We find that Mg vacancy can improve the thermodynamics. The energy cost to remove a hydrogen molecule from the vicinity of Mg vacancy is −0.73 eV. The negative sign means energy is gained if a hydrogen molecule is removed from the vicinity of the Mg vacancy and therefore the dehydrogenation process is exothermic. This energy cost is much less when compared with the energy cost of 2.9 eV to remove two hydrogen atoms from the vicinity of the Mg atom in intrinsic MgH_2.

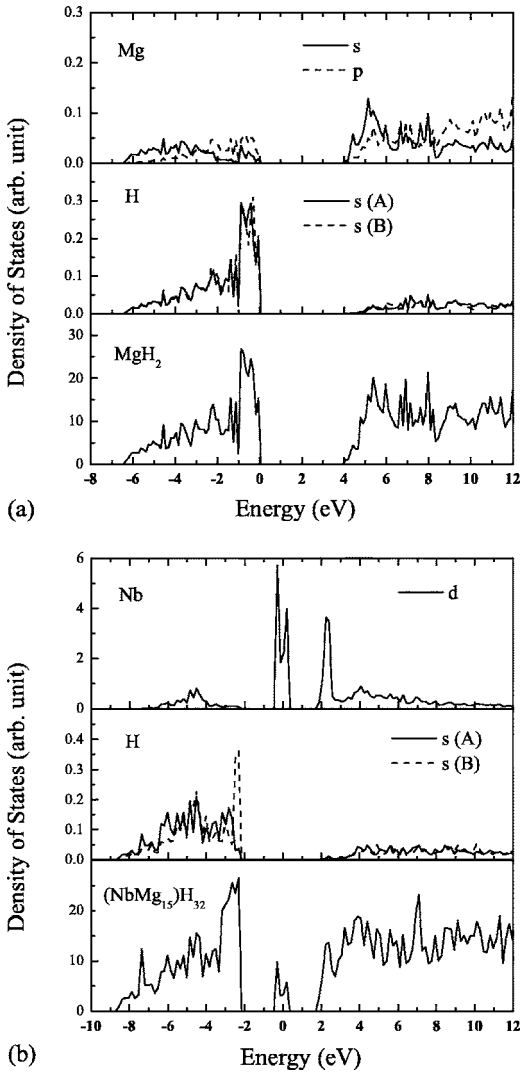

FIG. 2. (a) The s and p partial DOS of Mg, the s partial DOS of H atoms (both A and B in Fig. 3) and total density of states of $Mg_{16}H_{32}$ supercell are shown in the top, middle, and bottom panels, respectively. (b) The d partial DOS of Nb, the s partial DOS of H atoms (both A and B in Fig. 3) and total density of states of $(NbMg_{15})H_{32}$ supercell are shown in the top, middle, and bottom panels, respectively.

Since both Nb substitution as well as Mg vacancies play an important role in dehydrogenation, it is important to know the energies of their formation. The formation energy of a Nb atom substituted at the Mg site is calculated using the following equation:

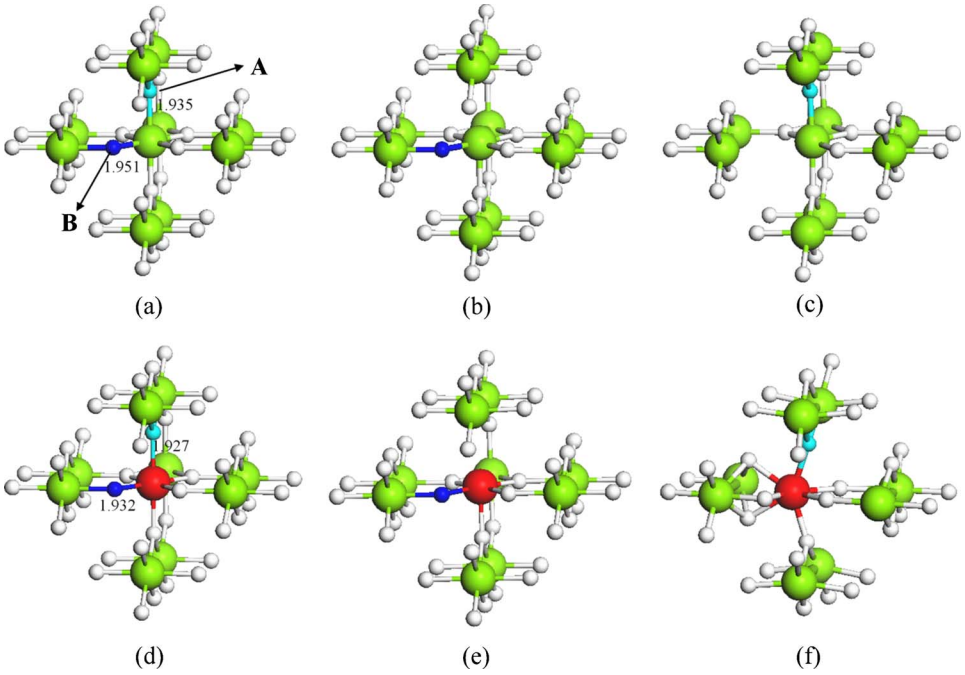

FIG. 3. (Color online) (a) The geometries of MgH_6 in the $Mg_{16}H_{32}$ supercell; (b) MgH_5 in the $Mg_{16}H_{31}$ supercell following the removal of the H atom marked *A* (c) same as in (b) except the H atom marked *B* is removed; (d), (e), and (f) the same legend as in (a), (b), and (c) except Mg is replaced by the Nb atom.

$$\Delta E = [E(\mathrm{NbMg_{15}H_{32}})_{\mathrm{coh}} + E(\mathrm{Mg_{hcp}})] - [E(\mathrm{Nb_{bcc}}) + E(\mathrm{Mg_{16}H_{32}})_{\mathrm{coh}}]. \quad (3)$$

The Mg vacancy formation energy was computed from the cohesive energies for $Mg_{16}H_{32}$ and $Mg_{15}H_{32}$ supercells using the following equation:

$$\Delta E_V = E(\mathrm{Mg_{15}H_{32}})_{\mathrm{coh}} + E(\mathrm{Mg_{hcp}}) - E(\mathrm{Mg_{16}H_{32}})_{\mathrm{coh}}. \quad (4)$$

The calculated vacancy formation energy is 3.87 eV, which is much higher than the 2.47 eV needed to substitute Nb at the Mg site. Thus, the Mg vacancy is less likely to play a role in dehydrogenation than the substitution of Nb at the Mg site because of high energy cost.

In summary, we have studied the dehydrogenation of MgH_2 by substituting Nb at the Mg site as well as by creating a Mg vacancy. Although both Nb substitution and metal vacancies are found to be effective in desorbing hydrogen at lower temperatures, the substitution of Nb at the Mg site is energetically more favorable than the formation of Mg vacancies. In particular, NbH_x cluster formation is observed directly following the Nb substitution. This supports the experimental conjecture that the existence of $(Nb, Mg)H_x$ solid solution following the addition of Nb_2O_5 catalysts is a likely pathway for dehydrogenation in MgH_2. We are currently studying the possibility that the formation of $(Nb,Mg)O_x$ complexes during the ball milling of MgH_2 with Nb_2O_5 may also promote dehydrogenation. These results will be published in due course.

This work was supported by grants from the Department of Energy (DOE), Swedish Research Council (VR), and by the Swedish Foundation for International Cooperation in Research and Higher Education (STINT).

[1] T. Vegge, Phys. Rev. B **70**, 035412 (2004).
[2] N. Hanada *et al.*, J. Alloys Compd. **366**, 269 (2004).
[3] G. Liang *et al.*, J. Alloys Compd. **292**, 247 (1999).
[4] W. Oelerich *et al.*, J. Alloys Compd. **315**, 237 (2001).
[5] T. Klassen *et al.*, J. Alloys Compd. **360–3**, 603 (2001).
[6] A. Zaluska *et al.*, Appl. Phys. A: Mater. Sci. Process. **72**, 157 (2001).
[7] A. Zaluska and L. Zaluski, J. Alloys Compd. **404**, 706 (2005).
[8] J. F. Pelletier *et al.*, Phys. Rev. B **63**, 052103 (2001).
[9] C. X. Shang *et al.*, Int. J. Hydrogen Energy **29**, 73 (2004).
[10] W. Oelerich *et al.*, J. Alloys Compd. **322**, L5 (2001).
[11] W. Oelerich *et al.*, Mater. Trans., JIM **42**, 1588 (2001).
[12] G. Barkhordarian *et al.*, Scr. Mater. **49**, 213 (2003).
[13] G. Barkhordarian *et al.*, J. Alloys Compd. **364**, 242 (2004).
[14] D. Fatay *et al.*, J. Alloys Compd. **399**, 237 (2005).
[15] Y. Song *et al.*, Phys. Rev. B **69**, 094205 (2004).
[16] D. Chen *et al.*, Acta Mater. **52**, 521 (2004).
[17] Z. Dehouche *et al.*, Nano Lett. **1**, 175 (2001).
[18] O. Friedrichs *et al.*, Acta Mater. **54**, 105 (2006).
[19] A. R. Yavari *et al.*, J. Alloys Compd. **353**, 246 (2003).
[20] J. F. R. de Castro *et al.*, J. Alloys Compd. **376**, 251 (2004).
[21] J. P. Perdew *et al.*, Phys. Rev. Lett. **77**, 3865 (1996).
[22] W. Kohn and L. J. Sham, Phys. Rev. **140**, A1133 (1965).
[23] P. E. Blochl, Phys. Rev. B **50**, 17953 (1994).
[24] G. Kresse and J. Furthmuller, Phys. Rev. B **54**, 11169 (1996).
[25] C. Kittel, *Introduction to Solid State Physics*, 7th ed. (Wiley, New York, 1995).
[26] F. I. Silvera, Rev. Mod. Phys. **52**, 393 (1980).
[27] A. B. Belonoshko *et al.*, Phys. Rev. Lett. **94**, 195701 (2005).
[28] P. Rulis *et al.*, Phys. Rev. B **71**, 235317 (2005).
[29] M. Bortz *et al.*, J. Alloys Compd. **287**, L4 (1999).
[30] P. Vajeeston *et al.*, Phys. Rev. Lett. **89**, 175506 (2002).
[31] R. Yu and P. K. Lam, Phys. Rev. B **37**, 8730 (1988).